Vinexin: A Novel Vinculin-binding Protein with Multiple SH3 Domains Enhances Actin Cytoskeletal Organization

Noriyuki Kioka,*‡ Shohei Sakata,‡ Takeshi Kawauchi,‡ Teruo Amachi,‡ Steven K. Akiyama,*§ Kenji Okazaki,‖ Christopher Yaen,* Kenneth M. Yamada,* and Shin-ichi Aota*‖

*Craniofacial Developmental Biology and Regeneration Branch, National Institute of Dental and Craniofacial Research, National Institutes of Health, Bethesda, Maryland 20892; ‡Laboratory of Biochemistry, Division of Applied Life Science, Kyoto University, Kyoto 606-01, Japan; §Laboratory of Molecular Carcinogenesis, National Institute of Environmental Health Science, Research Triangle Park, North Carolina 27709; and ‖Biomolecular Engineering Research Institute, Osaka 565-0874, Japan

Abstract. Using the yeast two-hybrid system and an in vitro binding assay, we have identified a novel protein termed vinexin as a vinculin-binding protein. By Northern blotting, we identified two types of vinexin mRNA that were 3 and 2 kb in length. Screening for full-length cDNA clones and sequencing indicated that the two mRNA encode 82- and 37-kD polypeptides termed vinexin α and β, respectively. Both forms of vinexin share a common carboxyl-terminal sequence containing three SH3 domains. The larger vinexin α contains an additional amino-terminal sequence. The interaction between vinexin and vinculin was mediated by two SH3 domains of vinexin and the proline-rich region of vinculin. When expressed, vinexin α and β localized to focal adhesions in NIH 3T3 fibroblasts, and to cell–cell junctions in epithelial LLC-PK1 cells. Furthermore, expression of vinexin increased focal adhesion size. Vinexin α also promoted upregulation of actin stress fiber formation. In addition, cell lines stably expressing vinexin β showed enhanced cell spreading on fibronectin. These data identify vinexin as a novel focal adhesion and cell–cell adhesion protein that binds via SH3 domains to the hinge region of vinculin, which can enhance actin cytoskeletal organization and cell spreading.

Key words: actin cytoskeleton • cell adhesion • focal adhesion • SH3 domain • vinculin

VINCULIN is an abundant cytoskeletal protein found in integrin-mediated cell-substrate adhesion sites (focal adhesions) and also in cadherin-mediated cell–cell adhesions (adherens junctions). Vinculin binds in vitro to cytoskeletal proteins such as talin, paxillin, α-actinin, and F-actin. By complex formation with these cytoskeletal proteins, vinculin is thought to contribute to organization of the actin cytoskeleton induced by integrin-meditated cell adhesion (Jockusch et al., 1995; Yamada and Geiger, 1997). Indeed, elevation or knock out of vinculin expression results in substantial alteration of cell adhesivity and motility (Rodríguez Fernández et al., 1993; Varnum-Finney and Reichardt, 1994; Coll et al., 1995; Goldmann et al., 1995; Volberg et al., 1995).

From studies with proteolytic fragments of vinculin and electron microscopy, vinculin appears to be composed of a large globular "head" domain and a rod-like "tail" domain (Milam, 1985; Molony and Burridge, 1985). The head domain binds to α-actinin and to talin, whereas the tail domain binds to F-actin and to the vinculin tail domain itself in an intermolecular interaction (for a review, see Jockusch et al., 1995). In the hinge region between the head and tail domains, vinculin has a short proline-rich sequence.

To date, many cytoskeletal proteins have been identified in focal adhesion and adherens junctions. Although numerous studies have elucidated the functions of these proteins and their interactions, little is known about the regulation of the topology of these interactions. Interestingly, the intramolecular interaction between the head and tail domain of vinculin has been suggested to modulate its interaction with the other cytoskeletal proteins, talin (Johnson and Craig, 1994), α-actinin (Kroemker et al., 1994), and F-actin (Johnson and Craig, 1995), as well as serine/threonine phosphorylation (Schwienbacher et al., 1996). Furthermore, phosphatidylinositol-4,5-bisphosphate (PIP2) has been found to dissociate vinculin's head–tail interaction, unmasking its talin- and actin-binding sites (Gilmore and Burridge, 1996; Weekes et al., 1996). Therefore, alteration of the conformation of vinculin is a potential regulatory mechanism for actin cytoskeletal changes.

Address correspondence to Shin-ichi Aota, Biomolecular Engineering Research Institute, Suita, 6-2-3 Furuedai, Osaka 565-0874, Japan. Tel.: 81-6-872-8208. Fax: 81-6-872-8219. E-mail: aota@beri.co.jp

Because of the potentially important location of the proline-rich region of vinculin and a high degree of sequence conservation of this region from *Caenorhabditis elegans* to human, we screened for binding proteins to this region using the yeast two-hybrid system. Here we report the identification and characterization of a novel vinculin-binding protein designated as vinexin.

Materials and Methods

Screening for a Vinculin-binding Protein

Two bait plasmids used for two-hybrid screening (Fields and Song, 1989; Chien et al., 1991), pGB410 and pGB411, contained the proline-rich region of chicken vinculin (see Fig. 1) fused with the GAL4 DNA-binding domain of pGBT9 (Clontech). The proline-rich region was amplified by PCR with primer pairs 409 (5′GCCGAATTCCAGCCTCAGGAGCCAGACTTTC3′) and 410 (5′GAAGTCGACTAATTGCTAGCTTCTCCTGCTTTC3′), 409 and 411 (5′CCCGTCGACTACTTGCTAGACCATTTCCGAGC3′), using a chicken vinculin cDNA clone as the template (kindly provided by Dr. Benjamin Geiger, The Weizmann Institute, Rehovot, Israel). The resulting PCR fragments were cut with EcoRI and SalI, and cloned into pGBT9.

The yeast strain HF7c (MATa, ura3-52, his3-200, ade2-101, lys2-801, trp-1-901, leu2-3, 112, gal4-542, gal80-538, LYS2::$GAL1_{UAS}$-$GAL1_{TATA}$-HIS3, URA3::$GAL4_{17mers(x3)}$-$CYC1_{TATA}$-lacZ) was transformed first with the bait plasmid, pGB410, and subsequently with a human placenta cDNA library (Clontech) fused to the GAL4 transcription-activating domain. Histidine autotrophic colonies were selected after incubation for 7 d on media plates lacking histidine, lysed in liquid nitrogen, and then assayed for β galactosidase activity on filters. The prey plasmids were recovered from the positive colonies and reintroduced into HF7c with pGB410, pGB411, or a control plasmid pLAM5′, which carries a human lamin C/GAL4 DNA binding domain hybrid in pGBT9 to exclude false positives.

To isolate full-length vinexin cDNA, a human HeLa 5′-stretch plus cDNA library (Clontech) and a mouse 13.5-d embryo cDNA library (kindly provided by Dr. Yoshihiko Yamada, National Institutes of Health [NIH], Bethesda, MD) were screened by plaque hybridization using the insert of the positive clone as a probe. The probe was labeled with ^{32}P using a randomly primed DNA labeling kit (Boehringer Mannheim).

Mapping of the Vinculin Binding Site

To map the vinculin binding site in the vinexin sequence, the yeast two-hybrid system was used to detect interactions between deletion mutants of vinexin and vinculin proline-rich regions. Primer pairs N1 (5′AATGAATTCGCCGCCAGGCTCAAGTTT3′) and C1 (5′AATGTCGACGGGCAGCACCTCCACATA3′), N2 (5′GAAGAATTCGAGGTTGTGGCCCAGT3′), and C2 (5′TATGTCGACTTCACGAGACACCTGC3′), and N1 and C2 were used for PCR to construct the plasmids pGAD1stSH3, pGAD2ndSH3, and pGAD1st2ndSH3, respectively. The resulting PCR products were digested with EcoRI and SalI and ligated into pGAD424 and sequenced. PCR was also used to amplify the deleted vinculin proline-rich region, pGB410d1 and pGB410d2, with primer pairs 729A (5′GCCGAATTCCATCTCCATCTGACTGATG3′) and 410, and 729B (5′AGAGAATTCCCAGAAGGTGAGGTTCCC3′) and 410, respectively. The PCR products were digested with EcoRI and SalI and subcloned into pGBT9.

After cotransformation of HF7c with the vinculin proline-rich region in pGBT9 and the vinexin deletion mutants in pGAD424, transformants were assayed for β galactosidase activity on filters or in solution.

In Vitro Binding Assay Using Affinity Precipitation

For an in vitro binding assay, various glutathione S-transferase (GST)[1] fusion proteins were expressed in *Escherichia coli* using the inserts of pGAD424 plasmids described above and GST expression plasmid pGEX-4T-1 (Pharmacia Fine Chemicals). To construct a GST fusion protein containing the first SH3 domain and a linker region between the two SH3 domains (clone pGAD1stSH3L), primer pairs N1 and CL (5′AATGTCGACTCCATACTCCAGCACCTG3′) were used for PCR, and the product was subcloned into pGEX-4T-1. GST fusion proteins were expressed in *E. coli* and purified with glutathione Sepharose 4B (Pharmacia Fine Chemicals) according to the supplier's instructions. Cultured human foreskin fibroblasts (kindly provided by Susan Yamada, NIH) were washed twice with PBS and lysed in NP-40 lysis buffer (0.5% NP-40, 100 μg/ml PMSF, 10 μg/ml aprotinin, 0.1 mM sodium orthovanadate). The lysate containing 400 μg total protein as estimated by microBCA assay (Pierce Chemical Co.) was incubated with 5 μg each of GST fusion protein and glutathione-Sepharose 4B at 4°C for 16 h. After four washes with lysis buffer, proteins were extracted from the Sepharose beads by boiling in loading buffer, resolved by 8% SDS-PAGE, and transferred to an Immobilon-P membrane (Millipore Corp.). Coprecipitated vinculin was detected by Western blotting using anti–human vinculin monoclonal antibody VII-F9 (a kind gift of Dr. Victor Koteliansky, Biogen, Inc., Cambridge, MA).

Northern Blotting

The cDNA of vinexin was labeled as described above and used to probe the human multiple tissue Northern blot (Clontech) containing 2 μg of polyA+ RNA.

Production of Polyclonal Antibody

Rabbit antiserum was raised against a recombinant vinexin fragment expressed by histidine-tagged bacterial expression vector pET22a (Novagen, Madison, WI) containing the vinexin cDNA insert of the clone (pVBP) isolated by the yeast two-hybrid screening. Polyclonal antibodies were affinity-purified using the recombinant protein covalently conjugated to Affigel 10 (Bio-Rad Laboratories). The bound antibodies were subsequently passed through an Affigel 10 column conjugated with *E. coli* whole protein extract to remove nonspecific antibodies.

Cell Lines

NIH 3T3, HeLa, C2C12, and LLC-PK1 cells were originally obtained from American Type Culture Collection and maintained in our laboratory. Mouse myoblastic C2C12 cells (Yaffe and Saxel, 1977) were induced to differentiate to myotubes by culturing with 10% horse serum for 6 d. Porcine kidney epithelial LLC-PK1 cells (Tanigawara et al., 1992) form a highly polarized monolayer, and were used to test vinexin localization in an epithelial cell.

Western Blotting

Cells were extracted with lysis buffer (1.0% Triton X-100, 1.0% sodium deoxycholate, 0.1% SDS) containing 100 μg/ml PMSF, 10 μg/ml aprotinin, 10 μg/ml leupeptin, and 2.5 mM EGTA. Extracted proteins (80 μg) were boiled in loading buffer for 3 min, resolved by 8% SDS-PAGE, and transferred to an Immobilon-P membrane. The filter was blocked with Block Ace (Dainippon Pharmaceutical), incubated with 0.66 μg/ml affinity-purified anti–vinexin antibody for 1 h, rinsed in TBS (100 mM Tris, pH 7.5, 150 mM NaCl) containing 0.1% Tween 20. Immune complexes were visualized with goat anti–rabbit IgG horseradish peroxidase–conjugated secondary antibody (Bio-Rad Laboratories) and developed using the ECL kit (Amersham International).

Subcellular Localization of Vinexin

Mouse vinexin α and β were tagged with Green Fluorescent Protein (GFP) or FLAG epitope (Eastman Kodak Co.) at the amino termini using the expression plasmids pGZ21 or p401F, respectively. pGZ21 contains a cytomegalovirus promoter and a GFP coding sequence with three amino acid residue substitutions (S65A, V68L, and S72A) to increase its fluorescence in mammalian cells (Cormack et al., 1996). Plasmid p401F is similar to pGZ21, but contains the FLAG epitope instead of GFP, and a neomycin-resistance gene for G418 selection. To construct the expression plasmid for the GFP-tagged amino-terminal half of vinexin α (pGFPVxH), an internal AccI restriction site was used to delete the carboxy-terminal half of vinexin α. PCR was used to amplify the DNA fragment for the third SH3 domain to construct pGFP3rdSH3.

NIH 3T3 cells were plated on coverslips 24 h after transfection of the expression plasmids using LipofectAMINE (Life Technologies, Inc.). We routinely observed that ~10–40% of the treated cells expressed vinexin or

1. *Abbreviations used in this paper:* GFP, green fluorescent protein; GST, glutathione S-transferase; VASP, vasodilator-stimulated phosphoprotein.

its fragments directed by each respective expression plasmid. After 24 h further incubation, the cells were fixed in 4% paraformaldehyde and 5% sucrose in PBS+ (PBS with 0.87 mM $CaCl_2$, 0.49 mM $MgCl_2$) for 30 min, and permeabilized for 5 min in 0.4% Triton X-100 in PBS+. The cells were blocked with 10% goat serum in PBS+ for 1 h, followed by incubation with antivinculin antibody. The cells were then stained with Texas Red–labeled sheep anti–mouse IgG anti-body (Amersham International) for 1 h. For F-actin staining, rhodamine-phalloidin (Molecular Probes, Inc.) was used. The fluorescence images were photographed by an Axiovert fluorescent microscope equipped with epifluorescence (Carl Zeiss Jena). For observing GFP fluorescence, a filter set for FITC supplied by Carl Zeiss Jena was used. The confocal microscope images were obtained using a Fluoview Confocal Laser Scanning microscope (Olympus Corp.).

Cell-spreading Assay

FLAG-tagged vinexin expression plasmids were constructed using the vector p401F described above. Geneticin at 800 μg/ml (Life Technologies, Inc.) was added to C2C12 cells 48 h after transfection with expression plasmids for FLAG-tagged vinexin α, vinexin β, or p401F alone. Geneticin-resistant clones expressing vinexin were selected and assayed by Western blotting. In a cell-spreading assay (Aota et al., 1994), cells were allowed to adhere and spread for 1 h on human plasma fibronectin coated at 1 μg/ml.

Results

Cloning and the Tissue Distribution of Vinexin

We used the proline-rich region of chicken vinculin for bait plasmids in the yeast two-hybrid method (Fig. 1), and screened a cDNA library constructed from human placenta polyA+ RNA. Four positive clones were isolated from 2×10^6 transformants. All four clones had an identical 1 kb cDNA fragment, and were designated pVBP. The insert of the clone contained two SH3 domains. We used the insert of pVBP as a probe for further screening to isolate full length cDNA clones, and for Northern blotting.

As shown in Fig. 2, we detected two types of mRNA molecules by Northern blotting that were 3 and 2 kb in length. The two mRNA species showed varying levels of expression in different human tissues. The 2-kb mRNA molecule was generally expressed at higher levels than the 3-kb molecule, and an especially high expression level was detected in heart for the 2-kb molecule. In contrast, a high expression level of the 3-kb molecule was observed in skeletal muscle. Interestingly, vinculin expression levels roughly correlated with the combined expression levels of the two types of vinexin mRNA molecule (Fig. 2).

When cDNA library screening was performed with pVBP as the probe, we were able to isolate only the 2-kb type of cDNA from HeLa cells. This result was consistent with the results of Northern blotting, where the 3-kb type of vinexin was not detected in HeLa cells (data not shown). We isolated 3-kb–type cDNA clones from a mouse embryo cDNA library. A schematic representation of these clones is shown in Fig. 3 A. The longer clone, p3A9, encodes an open reading frame of 82 kD, whereas the protein size predicted from the 2-kb–type cDNA clones is 37 kD. We designated these two proteins vinexin α and β, respectively. Vinexin β corresponds to the car-

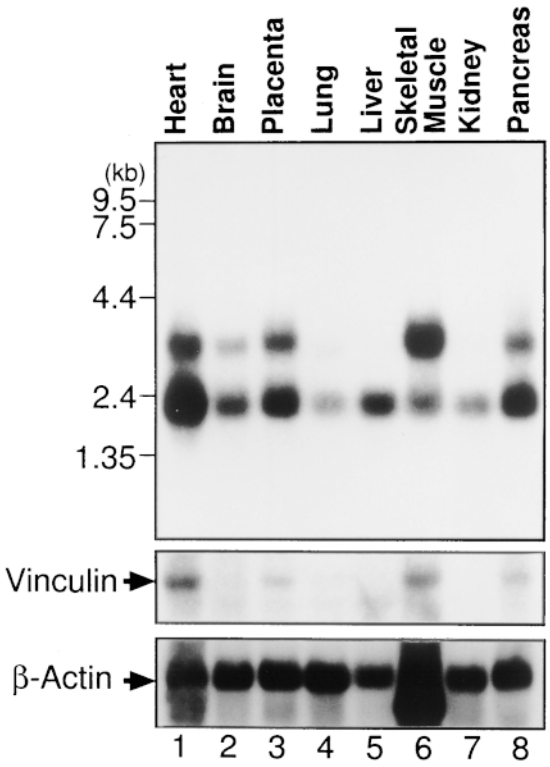

Figure 2. Northern blotting using vinexin cDNA. The insert of plasmid pVBP was labeled with ^{32}P and hybridized with polyA+ RNA resolved by electrophoresis and transferred to a Nylon membrane. Autoradiography of the blot is shown with the mobilities and sizes of molecular weight markers. The tissue sources of the polyA+ RNA are indicated along the top. Northern blotting patterns of vinculin and actin are also shown.

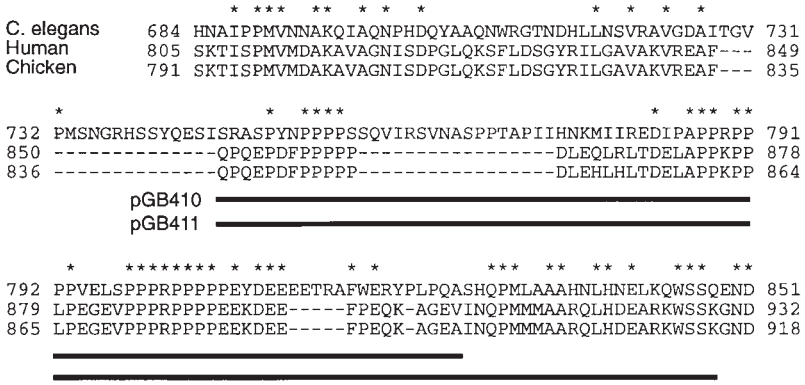

Figure 1. Construction of bait plasmids. The sequences from the vinculin proline–rich region used for bait plasmids are indicated by the black bars along with an alignment of vinculin sequences from *C. elegans*, human, and chicken. The asterisks indicate the amino acid residues conserved among these species. The numbers indicate the positions of the corresponding amino acid residues from each amino-terminal end.

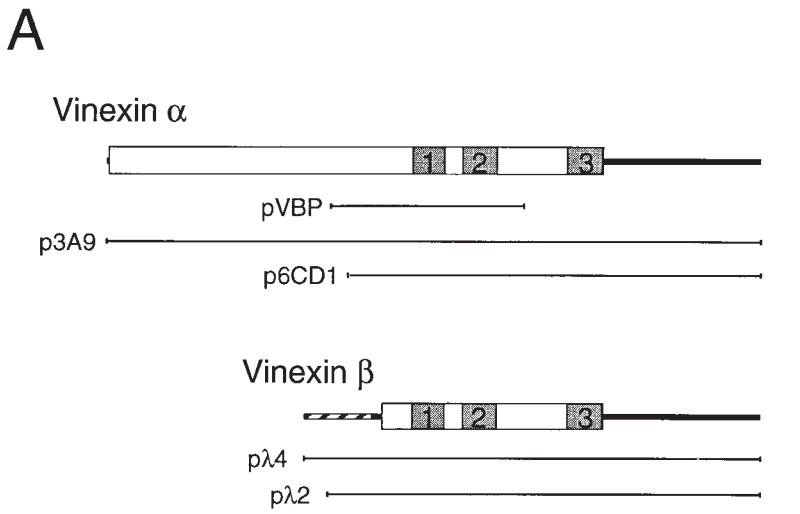

B

```
MARILGVGRSSASSLNNKEDNESDVALLSPKDPNRVHTKEQLAHPASSNLDPSMQGLPAG  60
LSLDDFIPGHLRTHIGSSSRGTRVPVIRNGGSNTLNFQFHDPAPRTVCNGCPPPRRDGSL 120
NPDPAWYQTWPGPGSRPSMSPKPPASQHAQNWSATWTKDSKRQDKRWVKYEGIGPVDESG 180
MPIAPRSSVDSPRDWYRRMFQQIHRKMPDLQLDWTLEDPPKVVSARASSAEPRHLGTLQR 240
PASRPGTTETSSGRNWNHSEETSRNTFNYNFRPSSSGLHPPNQVPRHREKVENVWTEDSW 300
NQFLHELETGHKPKKPLVDDPVEKPAQPIEVLLERELAKLSAELDKDLRAIETRLPSPKN 360
SQAPRRPLEQPGLEQQPSARLSSAWRPNSPHAPYFSSSRPLSPHRMADGGGSPFLGRRDF 420
                                        ↳
VYPSSAREPSASERGSSPSRKEEKKRKAARLKFDFQAQSPKELSLQKGDIVYIHKEVDKN 480
WLEGEHHGRLGIFPANYVEVLPADEIPKPIKPPTYQVLEYGDAVAQYTFKGDLEVELSFR 540
KGERICLIRKVNEHWYEGRITGTGRQGIFPASYVQINREPRLRLCDDGPQLPASPNPTTT 600
AHLSSHSHPSSIPVDPTDWGGRTSPRRSAFPFPITLQEPRSQTQSLNTPGPTLSHPRATS 660
RPINLGPSSPNTEIHWTPYRAMYQYRPQNEDELELREGDRVDVMQQCDDGWFVGVSRRTQ 720
KFGTFPGNYVAPV 733
```

Figure 3. Schematic diagram of domain organization of vinexin and its predicted amino acid sequence. (A) The open reading frame of vinexin is shown by open boxes. The grey boxes within the open reading frame indicate the three SH3 domains, and they are numbered sequentially from the amino terminus. The approximate position of each cDNA clone is shown by a line with its name under the corresponding schematic representation of each type of mRNA molecule. The 5′ end sequence unique to vinexin β is shaded with diagonal stripes, and is located at the 5′ untranslated region of vinexin β. (B) The 733 amino acid open reading frame contains three SH3 domains, indicated by boxes. The predicted amino-terminal end of vinexin β is shown by the arrow. A sequence motif search identified the three SH3 domains and a potential nuclear localization signal (underlined), although the importance of the latter is not clear at present. The nucleotide sequence data are available from Genbank/EMBL/DDBJ under accession Nos. AF064806 and AF064807.

boxyl-terminal half of vinexin α (Fig. 3 B). Since the 5′ end of the untranslated region of the cDNA clones from HeLa cells has a unique sequence not found so far in vinexin α cDNA clones, it is likely that two distinct alternative promoters give rise to the two different mRNA molecules.

To confirm that vinexin was actually expressed as expected, cultured cell lines were extracted with RIPA buffer, and Western blotting was performed with antivinexin polyclonal antibody. In NIH 3T3, HeLa, and LLC-PK1 cells, a protein band with an estimated mol wt of 38 kD was detected, suggesting that vinexin β is the major form in these cells (Fig. 4). In mouse myoblastic C2C12 cells, both vinexin α and β were detected. Interestingly, down-regulation of vinexin β was detected after induction of C2C12 differentiation. In HeLa and differentiated C2C12 cells, additional bands of ~30 and 75 kD were detected, indicating that there may be additional subtypes of vinexin, or, less likely, protein degradation.

Mapping of Vinculin Binding Site of Vinexin

Vinexin α and β share a common carboxyl-terminal sequence that contains the three SH3 domains. Clone pVBP isolated by the yeast two-hybrid screening contains the first and second SH3 domains (Fig. 3). To map the region for vinculin binding, various segments of vinexin were fused with the GAL4 activation domain in the plasmid pGAD424 (Fig. 5 A). They were introduced into the yeast strain HF7c with plasmid pGB410, which contains the proline-rich region of vinculin fused with the GAL4 DNA-binding domain. The results of β galactosidase activity assays for each clone are shown in Fig. 5 B. Vinculin binding

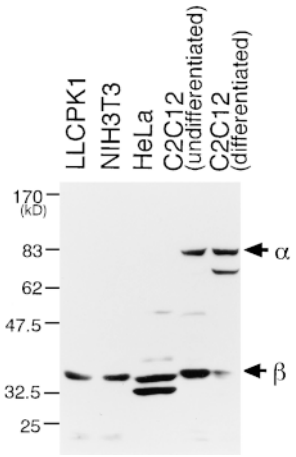

Figure 4. Western blotting pattern of vinexin. Protein samples extracted from LLC-PK1, HeLa, NIH 3T3, undifferentiated C2C12, and differentiated C2C12 cells were resolved by SDS-PAGE. This figure shows their Western blotting patterns using affinity-purified polyclonal antibody prepared against a recombinant vinexin fragment. Note that at least in HeLa and differentiated C2C12 cells there are additional bands other than vinexin α and β (see text).

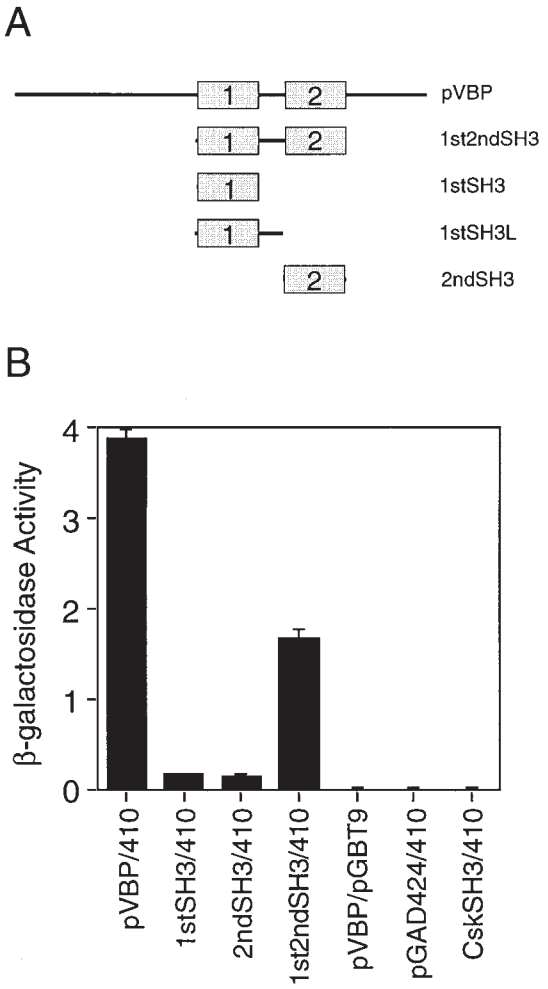

Figure 5. Vinculin–vinexin interaction assayed by β galactosidase activity in the yeast two-hybrid system. (A) A schematic diagram of deletion constructs is presented. The DNA fragments containing the first and/or second SH3 domain were amplified by PCR using appropriate primers, cloned in plasmid pGAD424 or pGST4T-1, and sequenced. The numbered gray boxes indicate the first and second SH3 domains of vinexin, respectively. (B) The activities of β galactosidase (in arbitrary units) in the lysate of each combination of bait and prey plasmids are shown. (410) pGB410, which contains the proline-rich region of vinculin in plasmid pGBT9, used for the bait plasmid. (CskSH3) pGAD424-based plasmid with the SH3 domain of Csk, included as a control. The experiment was repeated three times independently, and the averages and SD are shown.

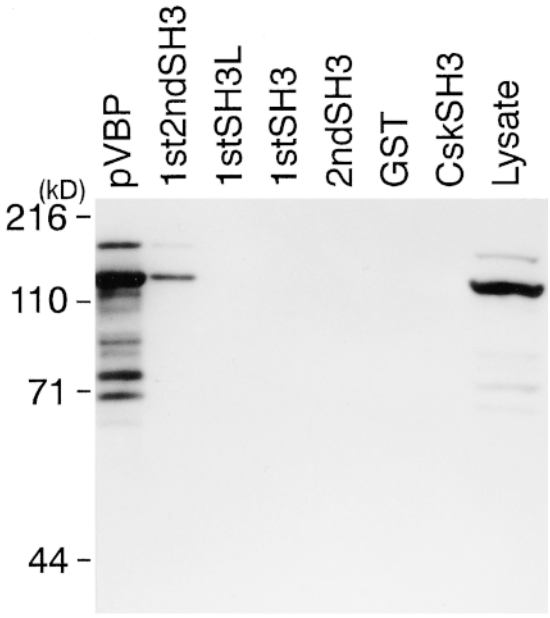

Figure 6. In vitro binding assay of vinculin–vinexin interaction. Protein extract from cultured human foreskin fibroblasts was incubated with GST fusion proteins with various parts of vinexin (Fig. 5) and glutathione-Sepharose beads as described in Materials and Methods. After extensive washing, proteins extracted from the beads were analyzed by Western blotting using antivinculin monoclonal antibody VII-F9. The GST fusion proteins corresponding to each lane are indicated along the top. See Fig. 5 A for a schematic diagram of these plasmids.

was not detected with either the first or second SH3 domain alone, whereas the clone with the first two SH3 domains showed vinculin binding.

The results of the two-hybrid assays were consistent with the results from an in vitro binding assay using GST fusion proteins. In this experiment, various parts of vinexin were expressed in *E. coli* as GST fusion proteins and were then bound to glutathione beads. The beads were incubated with cell lysate, washed, and then eluted fractions were analyzed by Western blotting using antivinculin antibody. As shown in Fig. 6, the first or the second SH3 domain alone, or the first SH3 domain with linker region (1stSH3L, Fig. 5 A) could not bind vinculin, whereas the clone containing the two SH3 domains bound vinculin in vitro. Thus, the minimal vinculin binding site was mapped to a region extending from the first to the second SH3 domain of vinexin. The binding activity of this minimal region was less than that of pVBP. One possible explanation is that the 5′ end region of pVBP may have an additional activity (discussed later), and another is that the GAL4 DNA-binding domain or GST is fused too close to the first SH3 domain in these clones.

Mapping of Vinexin-binding Site

To map the vinexin-binding site within the proline-rich region of vinculin more precisely, new bait plasmids with various parts of the proline-rich region were constructed (Fig. 7 A). The amino acid sequence from the 849th to 893rd amino acid residues of chicken vinculin (pGB410d1) showed vinexin binding in this experiment, but residues 866–893 (pGB410d2) did not (Fig. 7 B). Thus, the vinexin-binding site is within residues 849–893. This vinexin-binding region is especially well conserved from *C. elegans* to human (48% identity, Fig. 1).

Expression of Vinexin

To determine the subcellular localization of vinexin, GFP-tagged vinexin α and β (Fig. 8) were transfected into NIH 3T3 cells. The subcellular localization of vinexin was observed by GFP fluorescence, and the same cells were also

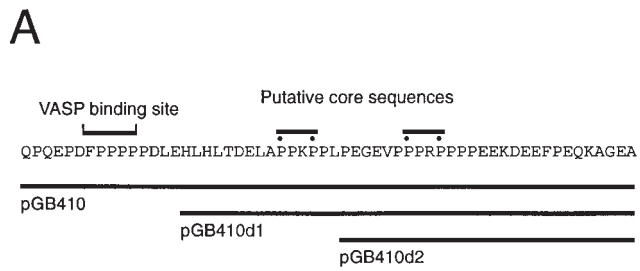

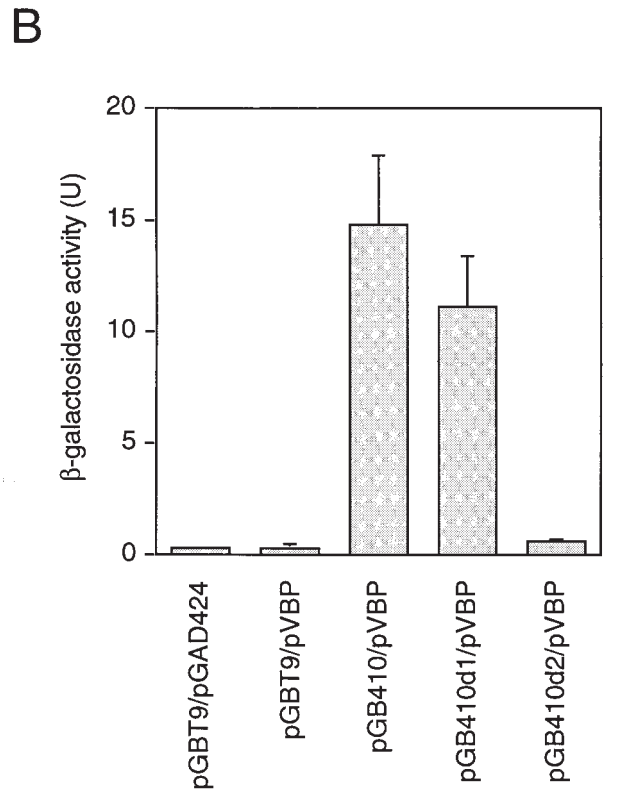

Figure 7. Deletion analysis of the vinculin proline-rich region. Three cDNA fragments from the chicken vinculin proline-rich region were cloned in pGBT9 (pGB410, pGB410d1, pGB410d2) and assayed for interaction with the vinculin binding region of vinexin using the yeast two-hybrid system. (A) Sequences of the fragments are indicated by the black lines along the sequence of vinculin (836–893). The VASP binding site (Brindle et al., 1996; Reinhard et al., 1996) is also shown. Two putative SH3-binding core sequences are also indicated with dots marking the conserved proline residues (see Discussion). (B) The yeast strain HF7c was transformed with each pair of plasmids and assayed for β galactosidase activity, shown here in arbitrary units. pVBP contains the 1-kb insert of vinexin initially isolated by the yeast two-hybrid screening in pGAD424, which is the original plasmid without an insert. The experiment was repeated three times, and means and SD are shown.

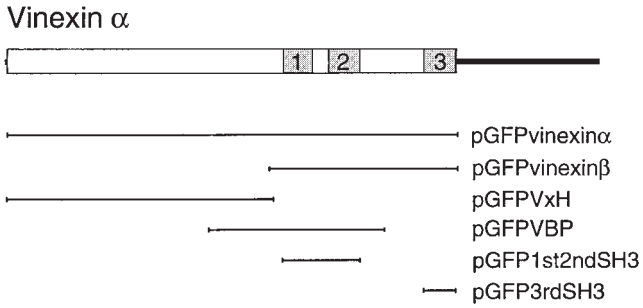

Figure 8. Construction of expression plasmids. A schematic diagram of vinexin α is presented at the top. The open reading frame for vinexin α is shown by the open box. Three SH3 domains are indicated by grey boxes numbered sequentially from the amino terminus. The approximate position of each DNA fragment is shown by a line with its name. The GFP coding sequence is fused in frame to the 5′ end of each clone.

stained with antivinculin monoclonal antibody VII-F9 and a Texas Red–labeled second antibody (Fig. 9). Both GFP-fused vinexin isoforms were predominantly localized at focal adhesions, and both colocalized with endogenous vinculin, although vinexin β was also found in the cytoplasm and sometimes in the nucleus. In NIH 3T3 cells highly expressing GFP-vinexin α, we sometimes observed vinculin-free dot-like GFP fluorescence, which is apparently aggregation of overexpressed GFP-vinexin α fusion protein (Fig. 9, A and B). FLAG-tagged vinexin α and vinexin β also localized to focal adhesions, and nontagged vinexin (expressed using clone p3A9) was also detected at focal adhesions by indirect immunostaining with antivinexin polyclonal antibody (data not shown). Thus, vinexin is a novel focal adhesion protein, and it colocalizes with vinculin. Interestingly, increased vinculin staining in focal adhesions was observed in the cells expressing vinexin α (Fig. 9, A and B). This finding may indicate the ability of vinexin α to recruit vinculin from the diffuse pool to focal adhesions, or to stabilize vinculin in focal adhesions.

Since vinculin can be found in cell–cell adhesions, vinexin localization in the porcine epithelial cell line LLC-PK1 was examined. As shown in Fig. 9, G and I, vinexin α and β were detected at cell–cell adhesions. For unknown reasons, the fluorescence levels of diffuse vinexin α and β were high, and vinexin α was often aggregated in LLC-PK1 cells.

Vinexin α–expressing cells also showed unusually strong rhodamine-phalloidin staining at focal adhesions, so that the actin stress fibers had swollen ends in these cells. This effect was particularly clearly observed by confocal microscopy, as shown in Fig. 10. The actin stress fibers in vinexin α–expressing cells were often stained strongly with rhodamine-phalloidin, though it was difficult to quantitate. In vinexin β–expressing cells, modest increases in size of focal adhesions were also observed (Fig. 10, G–I). Similar results were obtained with FLAG-tagged vinexin α and β (data not shown). In cells that expressed vinexin at high levels, aggregations of GFP fluorescence or FLAG indirect immunostaining were sometimes observed that lacked colocalized actin (Fig. 10, D and F).

Since vinexin may have several structural domains, various parts of vinexin were expressed separately (Fig. 8) and examined for subcellular localization (Fig. 11). As expected, the GFP-fused insert of pVBP containing the two SH3 domains required for vinculin binding localized to fo-

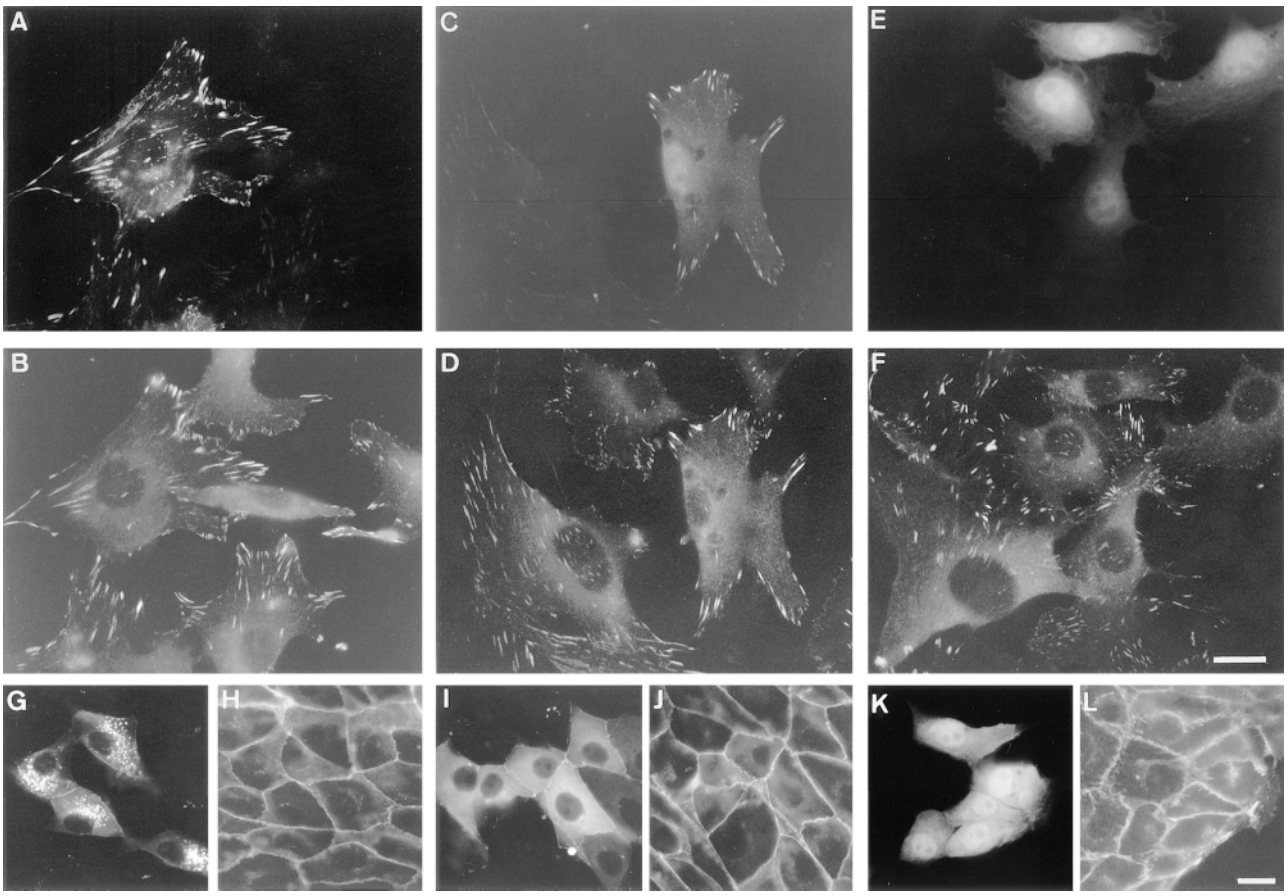

Figure 9. Subcellular localization of vinexin. GFP-tagged vinexin α (A and B), β (C and D), and GFP (E and F) were each transfected into NIH 3T3 cells. Vinexin-expressing and nonexpressing cells were examined for GFP fluorescence (A, C, and E) and indirect immunofluorescence labeling for vinculin (B, D, and F). Note the presence of vinculin-free GFP fluorescent dots in NIH 3T3 cells highly overexpressing GFP-vinexin α (A), suggesting aggregation of the fusion protein. GFP-tagged vinexin α (G and H), β (I and J), and GFP (K and L) were also transfected into epithelial LLC-PK1 cells. Vinexin-expressing and nonexpressing cells were observed for GFP fluorescence (G, I, and K) and indirect immunofluorescence labeling for β catenin (H, J, and L). Note that vinexin α is often aggregated in the cytoplasm of LLC-PK1 cells. The scale bar indicates 20 μm.

cal adhesions. GFP-fused minimal vinculin binding domain (pGFP1st2ndSH3) showed similar localization (data not shown). In contrast, the carboxyl-terminal SH3 domain (pGFP3rdSH3) showed a diffuse pattern of localization. Interestingly, the amino-terminal half of vinexin α (pGFPVxH) was also localized in focal adhesions in NIH 3T3 cells (Fig. 11), indicating the existence of focal adhesion–binding activity in this domain. In contrast to vinexin α, expression of the amino-terminal half of vinexin α did not change actin cytoskeletal organization (data not shown).

Expression of Vinexin Enhances Cell Spreading

Since vinexin appeared to be a novel protein of focal adhesions, we examined the effect of vinexin expression on cell spreading on a fibronectin substrate. Two stably expressing clones of C2C12 cells with vinexin β were isolated and assayed for cell-spreading activity. As shown in Fig. 12, vinexin β–expressing cells showed enhanced cell spreading on fibronectin substrates compared with mock transfectants and untreated C2C12 cells. For unknown reasons, we have not yet been able to isolate stable vinexin α–expressing C2C12 cells, or vinexin α– and β–expressing NIH 3T3 cells.

Discussion

We have identified and characterized a novel SH3 domain-containing protein termed vinexin. The vinculin-binding sequence of vinexin was mapped within the region extending from the first SH3 domain to the second using the yeast two-hybrid system and an in vitro binding assay. This mapping result was consistent with the results obtained in the vinexin-expression experiments, in which vinexin α and β and the vinculin-binding region were expressed in NIH 3T3 cells: all resulted in localizations at focal adhesions. They also localized to cell–cell adhesions in epithelial LLC-PK1 cells. Expression of vinexin α also promoted an increase in vinculin staining at focal adhesions. These results were consistent with the notion that

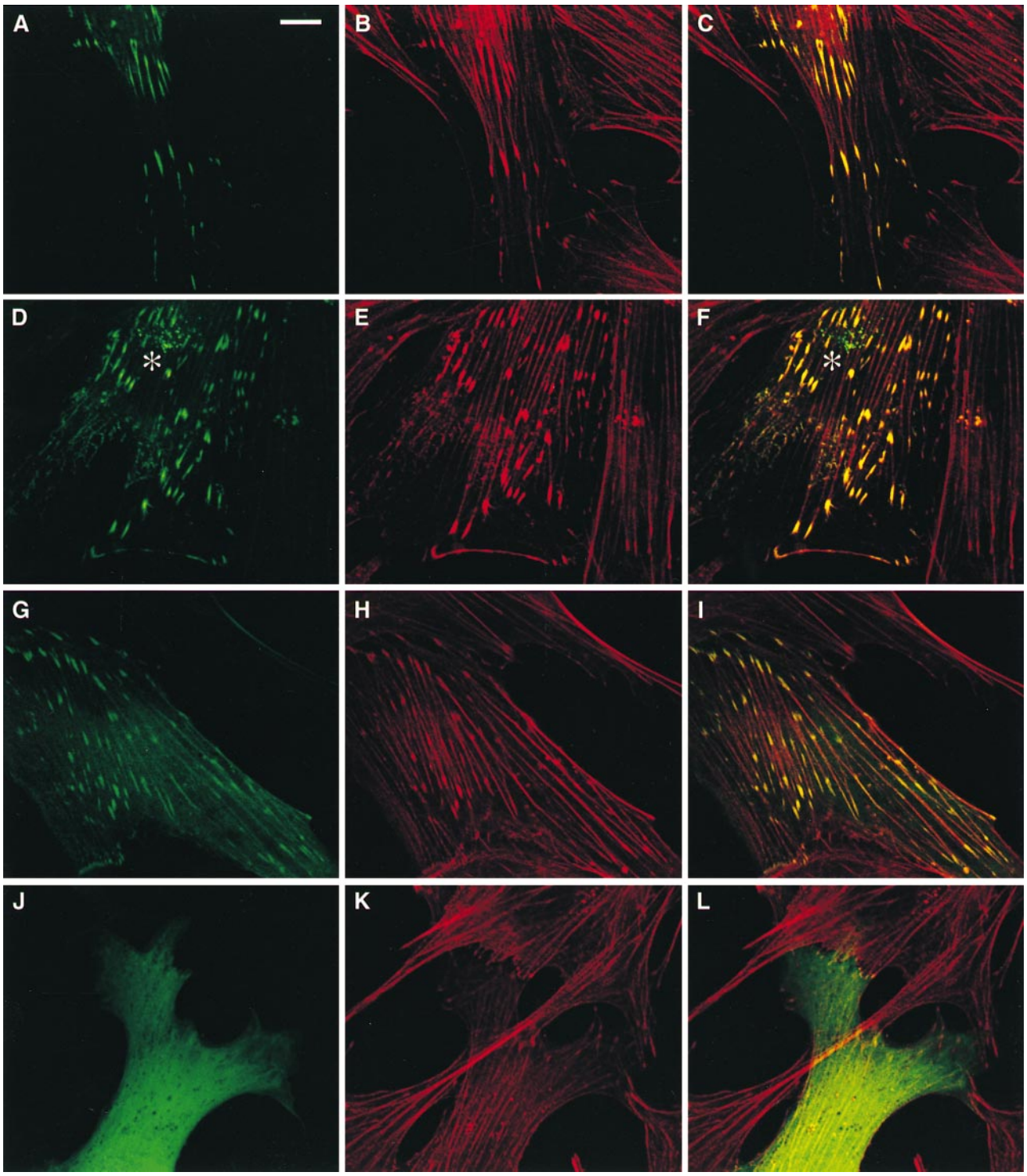

Figure 10. Confocal microscope images of cells expressing vinexin. Confocal images of an NIH 3T3 cell expressing GFP-tagged vinexin α and nonexpressing cells, as observed by GFP fluorescence (A), rhodamine-phalloidin (B), and overlaid GFP and rhodamine fluorescence (C). The scale bar indicates 10 μm. Note that strong rhodamine-phalloidin staining was observed where GFP-tagged vinexin α was localized. A different set of images (D, E, and F) is also shown for cells highly expressing vinexin α. In high expressers, aggregations of GFP fluorescence were also observed (D and F, *). A vinexin β–expressing cell is shown by GFP fluorescence (G), rhodamine-phalloidin (H), and overlaid GFP and rhodamine fluorescence (I). Note the modestly strong rhodamine-phalloidin staining at focal adhesions. As a control, a cell expressing GFP alone is shown (J, K, and L). This confocal microscope optical section was at the ventral surface (bottom).

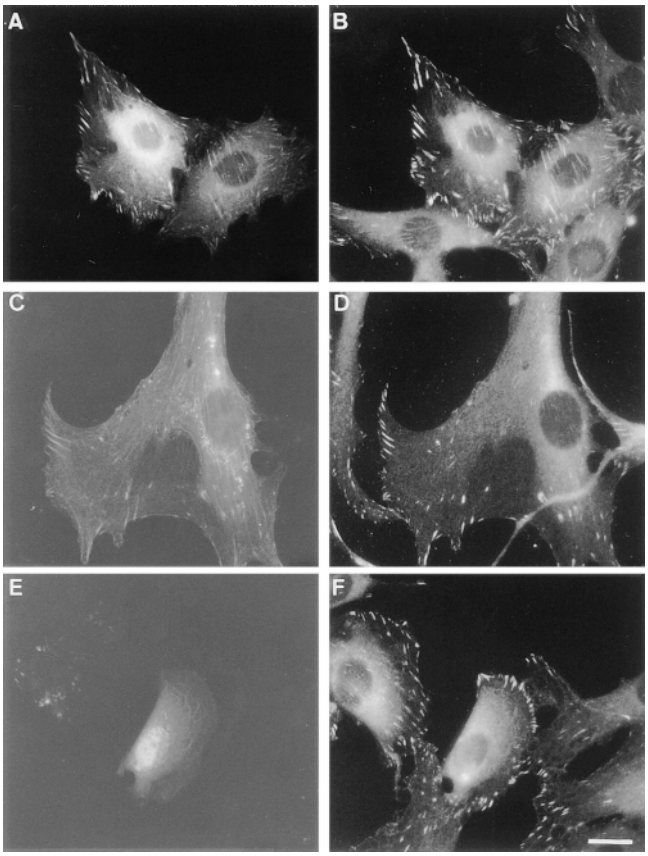

Figure 11. Subcellular localization of vinexin domains. GFP-tagged vinexin domains were expressed in NIH 3T3 cells, and the localization of each domain and vinculin were observed by GFP fluorescence and indirect immunofluorescent staining for vinculin. (A) GFP-tagged pVBP insert (pGFPVBP, see Fig. 8) was transfected and GFP fluorescence was photographed. (B) The same cells were also stained for vinculin localization. Cells transfected with the GFP–amino terminal domain of vinexin α (pGFPVxH) were observed for GFP (C) and vinculin (D) localization. GFP-tagged third SH3 domain–transfected cells (pGFP3rdSH3), observed by GFP (E) and vinculin (F). Bar, 20 μm.

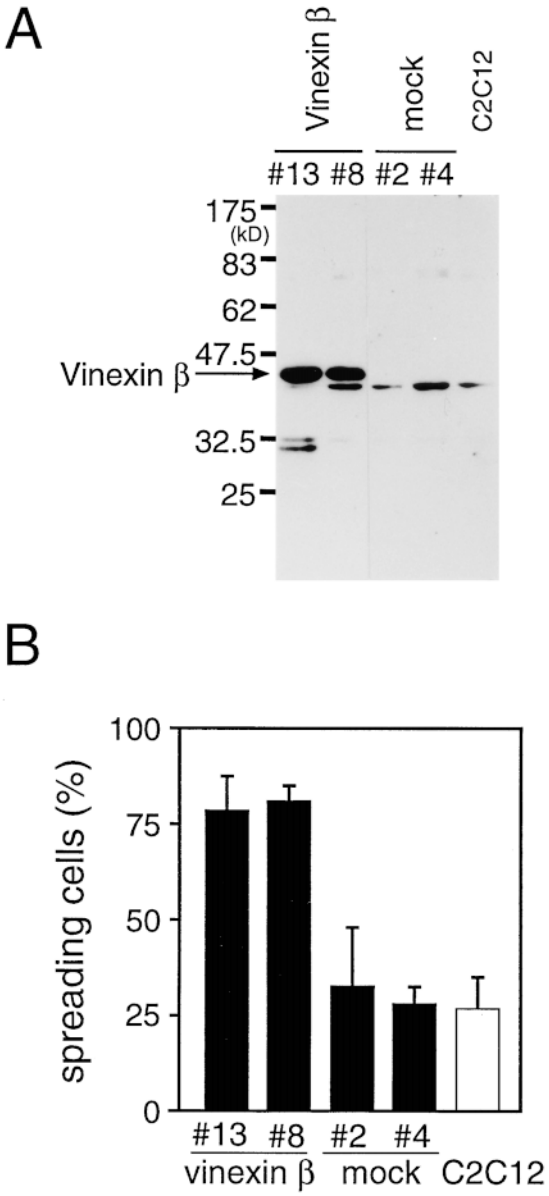

Figure 12. Effect of vinexin β expression on cell spreading. (A) Two stable clones of C2C12 cells (#13 and #8) expressing vinexin β were isolated. Two stable clones of mock-transfected cells (#2 and #4) using the expression vector (p401F) were included as controls. FLAG-tagged vinexin β was detected by Western blotting using anti–FLAG antibody. (B) The cell-spreading activities of these lines and mock transfectants were assayed by a cell-spreading assay using fibronectin-coated substrates. The percentages of cells that spread on fibronectin were determined and shown as mean ± SD.

vinexin binds to vinculin in vivo. Thus, we propose that vinexin is a novel vinculin-binding protein and also a novel component in focal adhesion and cell–cell adhesion.

We identified a novel binding sequence in the primary structure of vinculin. This vinexin-binding sequence was mapped within residues 849–893 of chicken vinculin. It is now well established that SH3 domains bind to proline-rich sequences of which the core sequence is "PXXP," where "P" is a proline residue and "X" for any amino acid other than cysteine (Cohen et al., 1995). As shown in Fig. 7 A, it is possible to assign a pair of putative PXXP motifs in the vinexin-binding region. Exact mapping of the vinexin-binding site remains to be determined. It is also noteworthy that a high level of sequence conservation throughout evolution of the vinexin-binding site of vinculin implies the importance of the interaction between vinculin and vinexin.

The specificity of interaction between single SH3 domain and the proline-rich motif has been studied extensively. To our knowledge, this is the first demonstration that a pair of SH3 domains is required for the specific interaction of two proteins, although a similar multivalency-dependent specificity has been proposed for the interaction between Sos and Grb2 (Lim, 1996). In the case of the SH2 domain, multivalency is known to raise the specificity of SH2 domain interactions of ZAP-70 (Hatada et al., 1995) and SH-PTP2 (Eck et al., 1996). This vinexin–vinculin interaction may provide a valuable insight into the

specificity of molecular recognition of multiple binding modules.

The proline-rich region of vinculin has been examined by several studies, and generally considered to be a hinge between the head and tail domains (Jockusch et al., 1995). There are two sites near the vinexin-binding region where V8 protease readily cleaves vinculin (Price et al., 1989). Thus, this region of vinculin is likely to be exposed on the surface of the molecule. It has been shown that the cytoskeletal protein vasodilator-stimulated phosphoprotein (VASP) binds to the adjacent proline-rich stretch (residues 842–846) of vinculin in vitro (Brindle et al., 1996; Reinhard et al., 1996). The binding site of VASP is therefore very close to, but not overlapping with, the vinexin binding sequence (Fig. 7 A). It will be interesting to determine whether VASP and vinexin can access the proline-rich region of vinculin concurrently or exclusively of each other.

Expression of vinexin α resulted in a significant increase in the size of focal adhesions and also an increase in actin stress fiber formation. Since the effects of vinexin β expression on actin cytoskeleton was not as conspicuous as vinexin α, the amino-terminal half of vinexin α (referred to hereafter as VxH domain) was suggeted to play roles in the upregulation of actin cytoskeletal organization. Our results also indicated that the VxH domain can bind to focal adhesions, since it became localized to cell adhesions when the domain alone was expressed in NIH 3T3 cells. Therefore, vinexin α contains multiple interaction sites to

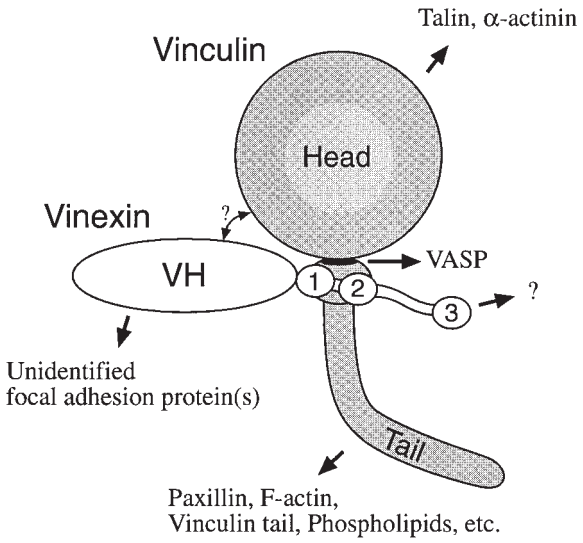

Figure 13. Schematic diagram of multiple binding sites of vinexin. A complex of vinexin and vinculin is depicted, with known or potential ligands of each domain indicated. VxH represents the amino-terminal half of vinexin α, suggested to bind to focal adhesions. The three SH3 domains of vinexin are shown (1, 2, and 3). The region extending from the first SH3 domain to the second was mapped as the vinculin binding sequence, although a portion of the VxH domain may also contribute to the interaction between vinexin and vinculin, as suggested by in vitro binding assay (see Results). Note that the overall shape of vinexin as depicted here is hypothetical, in contrast to the known shape of vinculin based on electron microscopic images. The binding site of VASP on vinculin is very close to the vinexin binding site.

focal adhesion components, as summarized in Fig. 13. The ligand(s) of the third SH3 domain is unknown at present. In contrast to the conspicuous effects on focal adhesions and stress fibers of vinexin α, expression of the VxH domain alone resulted in no apparent effect on focal adhesions and stress fibers. Thus, the VxH and the vinculin-binding domains may act cooperatively to upregulate actin cytoskeletal organization, although the exact molecular mechanism remains to be examined.

Our results indicate that vinexin is a novel component of focal adhesions with a capacity to interact with vinculin. Numerous studies have been focused on the assembly of integrin receptors, focal adhesion components, and actin microfilaments. Focal adhesions are large macromolecular assemblies, consisting of many proteins including vinculin, talin, α-actinin, paxillin, and actin. The interaction and assembly of the focal adhesion molecules are complex and highly cooperative processes in which they are efficiently recruited from diffusible pools within the cell and bound to each other to form multimolecular complexes linked to the actin cytoskeleton (Geiger et al., 1992; Jockusch et al., 1995; Yamada and Geiger, 1997; Burridge et al., 1997). At present, it is difficult to determine how vinexin α enhances these processes. It is, however, noteworthy that the effect of vinculin overexpression (Geiger et al., 1992) is similar to that of vinexin α; i.e., a significant increase in the size of focal adhesions and stress fibers. A possible cooperative recruitment of vinculin and vinexin α to focal adhesions, or stabilization of vinculin, may play an important role, since our results showed that vinculin staining at focal adhesions was markedly enhanced in vinexin α–expressing cells.

We found that the effect of vinexin β expression on actin cytoskeletal organization was less than that of vinexin α. Nevertheless, when stably transfected cells were assayed for cell-spreading activities on fibronectin, vinexin β–expressing clones showed significantly higher cell-spreading activities than did mock-transfected cell lines. Since conformational alteration of vinculin has been suggested as a mechanism for the modulation of vinculin function (Johnson and Craig, 1994, 1995; Kroemker et al., 1994; Schwienbacher et al., 1996), there is a possibility that vinexin β may enhance cell spreading by modulating vinculin conformation.

Homology searches of DNA and protein databases revealed two other structurally related proteins, CAP and ArgBP2. CAP, also known as SH3P12, was originally isolated as a binding protein to proline-rich sequences in a systematic screening experiment for SH3 domains (Sparks et al., 1996), and later as a binding protein to c-Cbl (Ribon et al., 1998b). ArgBP2 was isolated by a two-hybrid screening for Arg- and Abl-binding proteins (Wang et al., 1997). These two molecules and vinexin each contain three SH3 domains, and CAP and ArgBP2 are most related to each other at the sequence level. There are sequence homologies found in ArgBP2 and CAP with some stretches of amino acid sequence within the vinexin VxH domain. In contrast to vinexin, both CAP and ArgBP2 have been reported to localize with actin stress fibers. Recently, expression of CAP was reported to enhance actin stress fiber formation and focal adhesions, and association of CAP with cytoskeletal signaling molecules such as p125 FAK was

suggested (Ribon et al., 1998a). These differences between the two molecules and vinexin in subcellular localization and association partners may indicate related but diverse roles of these molecules.

We thank Drs. Mark De Nichilo, Benjamin Geiger, Victor Koteliansky, Yoshihiko Yamada, and Susan Yamada for providing valuable materials. We also thank Drs. Tohru Komano, Kazumitsu Ueda, and Yoshiro Shimura for helpful advice and support.

Received for publication 26 May 1998 and in revised form 16 November 1998.

References

Aota, S., M. Nomizu, and K.M. Yamada. 1994. The short amino acid sequence Pro-His-Ser-Arg-Asn in human fibronectin enhances cell-adhesive function. *J. Biol. Chem.* 269:24756–24761.

Brindle, N.P., M.R. Holt, J.E. Davies, C.J. Price, and D.R. Critchley. 1996. The focal-adhesion vasodilator-stimulated phosphoprotein (VASP) binds to the proline-rich domain in vinculin. *Biochem. J.* 318:753–757.

Burridge, K., M. Chrzanowska-Wodnicka, and C. Zhong. 1997. Focal adhesion assembly. *Trends Cell Biol.* 7:342–347.

Chien, C.T., P.L. Bartel, R. Sternglanz, and S. Fields. 1991. The two-hybrid system: a method to identify and clone genes for proteins that interact with a protein of interest. *Proc. Natl. Acad. Sci. USA*. 88:9578–9582.

Cohen, G.B., R. Ren, and D. Baltimore. 1995. Modular binding domains in signal transduction proteins. *Cell.* 80:237–248.

Coll, J.L., A. Ben-Ze'ev, R.M. Ezzell, J.L. Rodríguez Fernández, H. Baribault, R.G. Oshima, and E.D. Adamson. 1995. Targeted disruption of vinculin genes in F9 and embryonic stem cells changes cell morphology, adhesion, and locomotion. *Proc. Natl. Acad. Sci. USA.* 92:9161–9165.

Cormack, B.P., R.H. Valdivia, and S. Falkow. 1996. FACS-optimized mutants of the green fluorescent protein (GFP). *Gene*. 173:33–38.

Eck, M.J., S. Pluskey, T. Trub, S.C. Harrison, and S.E. Shoelson. 1996. Spatial constraints on the recognition of phosphoproteins by the tandem SH2 domains of the phosphatase SH-PTP2. *Nature.* 379:277–280.

Fields, S., and O. Song. 1989. A novel genetic system to detect protein–protein interactions. *Nature.* 340:245–246.

Geiger, B., O. Ayalon, D. Ginsberg, T. Volberg, J.L. Rodríguez Fernández, Y. Yarden, and A. Ben-Ze'ev. 1992. Cytoplasmic control of cell adhesion. *Cold Spring Harbor Symp. Quant. Biol.* 57:631–642.

Gilmore, A.P., and K. Burridge. 1996. Regulation of vinculin binding to talin and actin by phosphatidyl-inositol-4-5-bisphosphate. *Nature.* 381:531–535.

Goldmann, W.H., M. Schindl, T.J. Cardozo, and R.M. Ezzell. 1995. Motility of vinculin-deficient F9 embryonic carcinoma cells analyzed by video, laser confocal, and reflection interference contrast microscopy. *Exp. Cell Res.* 221: 311–319.

Hatada, M.H., X. Lu, E.R. Laird, J. Green, J.P. Morgenstern, M. Lou, C.S. Marr, T.B. Phillips, M.K. Ram, K. Theriault, M.J. Zoller, and J.L. Karas. 1995. Molecular basis for interaction of the protein tyrosine kinase ZAP-70 with the T-cell receptor. *Nature.* 377:32–38.

Jockusch, B.M., P. Bubeck, K. Giehl, M. Kroemker, J. Moschner, M. Rothkegel, M. Rudiger, K. Schluter, G. Stanke, and J. Winkler. 1995. The molecular architecture of focal adhesions. *Annu. Rev. Cell Dev. Biol.* 11:379–416.

Johnson, R.P., and S.W. Craig. 1994. An intramolecular association between the head and tail domains of vinculin modulates talin binding. *J. Biol. Chem.* 269:12611–12619.

Johnson, R.P., and S.W. Craig. 1995. F-actin binding site masked by the intramolecular association of vinculin head and tail domains. *Nature.* 373:261–264.

Kroemker, M., A.H. Rudiger, B.M. Jockusch, and M. Rudiger. 1994. Intramolecular interactions in vinculin control alpha-actinin binding to the vinculin head. *FEBS Lett.* 355:259–262.

Lim, W.A. 1996. Reading between the lines: SH3 recognition of an intact protein. *Structure.* 4:657–659.

Milam, L.M. 1985. Electron microscopy of rotary shadowed vinculin and vinculin complexes. *J. Mol. Biol.* 184:543–545.

Molony, L., and K. Burridge. 1985. Molecular shape and self-association of vinculin and metavinculin. *J. Cell. Biochem.* 29:31–36.

Price, G.J., P. Jones, M.D. Davison, B. Patel, R. Bendori, B. Geiger, and D.R. Critchley. 1989. Primary sequence and domain structure of chicken vinculin. *Biochem. J.* 259:453–461.

Reinhard, M., M. Rudiger, B.M. Jockusch, and U. Walter. 1996. VASP interaction with vinculin: a recurring theme of interactions with proline-rich motifs. *FEBS Lett.* 399:103–107.

Ribon, V., R. Herrera, B.K. Kay, and A.R. Saltiel. 1998a. A role for CAP, a novel, multifunctional Src Homology 3 domain-containing protein in formation of actin stress fibers and focal adhesions. *J. Biol. Chem*. 273:4073–4080.

Ribon, V., J.A. Printen, N.G. Hoffman, B.K. Kay, and A.R. Saltiel. 1998b. A novel, multifunctional c-Cbl binding protein in insulin receptor signaling in 3T3-L1 adipocytes. *Mol. Cell. Biol.* 18:872–879.

Rodríguez Fernández, J.L., B. Geiger, D. Salomon, and A. Ben-Ze'ev. 1993. Suppression of vinculin expression by antisense transfection confers changes in cell morphology, motility, and anchorage-dependent growth of 3T3 cells. *J. Cell Biol.* 122:1285–1294.

Schwienbacher, C., B.M. Jockusch, and M. Rudiger. 1996. Intramolecular interactions regulate serine/threonine phosphorylation of vinculin. *FEBS Lett.* 384:71–74.

Sparks, A.B., N.G. Hoffman, S.J. McConnell, D.M. Fowlkes, and B.K. Kay. 1996. Cloning of ligand targets: systematic cloning of functional SH3 domains. *Nat. Biotechnol.* 14:741–744.

Tanigawara, Y., N. Okamura, M. Hirai, M. Yasuhara, K. Ueda, N. Kioka, T. Komano, and R. Hori. 1992. Transport of digoxin by human P-glycoprotein expressed in a porcine kidney epithelial cell line (LLC-PK1). *J. Pharmacol. Exp. Ther.* 263:840–845.

Varnum-Finney, B., and L.F. Reichardt. 1994. Vinculin-deficient PC12 cell lines extend unstable lamellipodia and filopodia and have a reduced rate of neurite outgrowth. *J. Cell Biol.* 127:1071–1084.

Volberg, T., B. Geiger, Z. Kam, R. Pankov, I. Simcha, H. Sabanay, J.L. Coll, E. Adamson, and A. Ben-Ze'ev. 1995. Focal adhesion formation by F9 embryonal carcinoma cells after vinculin gene disruption. *J. Cell Sci.* 108:2253–2260.

Wang, B., E.A. Golemis, and G.D. Kruh. 1997. ArgBP2, a multiple Src homology 3 domain-containing, Arg/Abl-interacting protein, is phosphorylated in v-Abl-transformed cells and localized in stress fibers and cardiocyte Z-disks. *J. Biol. Chem*. 272:17542–17550.

Weekes, J., S.T. Barry, and D.R. Critchley. 1996. Acidic phospholipids inhibit the intramolecular association between the N- and C-terminal regions of vinculin, exposing actin-binding and protein kinase C phosphorylation sites. *Biochem. J*. 314:827–832.

Yaffe, D., and O. Saxel. 1977. Serial passaging and differentiation of myogenic cells isolated from dystrophic mouse muscle. *Nature.* 270:725–727.

Yamada, K.M., and B. Geiger. 1997. Molecular interactions in cell adhesion complexes. *Curr. Opin. Cell Biol.* 9:76–85.